Metal organic Framework Enhanced SPEEK/SPSF Heterogeneous Membrane for Ion Transport and Energy Conversion

Xiaolu Zhao [a, b], Chunxin Lu [c], Linsen Yang [a, b], Weipeng Chen [a, b], Weiwen Xin [a, b], Xiang-Yu Kong [a, b], Qiang Fu [d, *], Liping Wen [a, b, *], Greg Qiao [e], Lei Jiang [a, b]

[a] CAS Key Laboratory of Bio-inspired Materials and Interfacial Science, Technical Institute of Physics and Chemistry, Chinese Academy of Sciences, Beijing 100190, P R China

[b] University of Chinese Academy of Sciences, Beijing 100049, P R China.

[c] College of Biological, Chemical Sciences and Engineering Jiaxing University, Jiaxing 314001, P R China.

[d] The Centre for Technology in Water and Wastewater (CTWW), School of Civil and Environmental Engineering, University of Technology Sydney, NSW 2007 Australia

[e] Polymer Science Group, Department of Chemical and Biomolecular Engineering, The University of Melbourne, VIC 3010 Australia

* Corresponding author
Liping Wen: wen@mail.ipc.ac.cn; Qiang Fu: qiang.fu@uts.edu.au

ABSTRACT

Bioinspired nanofluidic devices have drawn increasing global interest due to their giant applicable potential in a wide range of fields. By mimicking biological prototype, it is expected to achieve high energy conversion efficiency and tunable ion transport. However, the low osmotic conversion efficiency, weak ion transport capability and poor mechanical performance limit practical application. We designed a class of heterogeneous membrane consisting of a support layer and a thin top layer to meet fundamental requirements. To achieve higher power generation, we incorporated metal organic framework (MOF) nanosheets (dispersed phase) into polymer matrix (continuous phase) to afford a mixed matrix top layer. This unique structure addressed the geometric restriction associated with the polymeric specie due to their limited pore accessibility. As a result, the presented membranes produced high power density of *ca.* 7 W m^{-2} and a high energy conversion efficiency of *ca.* 40% under a salinity gradient of 50 (0.5 M|0.01 M, NaCl). This work thus offers an insight into a new methodology in the development of a novel membrane technology for highly efficient energy conversion.

KEYWORDS: energy conversion, salinity gradient energy, mixed matrix membrane, metal organic framework

1. Introduction

Nature provides a unique perspective on power generation because organisms have efficient energy conversion and storage systems *via* ion transport.[1, 2] As ubiquitous phenomena in biology, it lays a solid foundation for complex physiological activity.[3] Typically, directional ion transport could generate more than 100 V electricity through

concentration gradient of electrolyte for eel.[4] The electricity directly generates from the Gibbs free energy of mixing through highly concentrated seawater and fresh through ion selective channel,[5, 6] which allows the counter ions to pass though the membrane preferentially, while compelling the common ions as much as possible. The migration of surplus ions thus results in a voltage difference between the two ends of channels. In addition, the ion channel could regulate ion fluxes, ion species and flow directions, which are so-called ion gating, ion selectivity and ion rectification, respectively. Bioinspired nanochannel membranes have been proposed to mimic such biological functions.[7, 8] However, an immediate challenge to achieve high energy conversion and fast ion transport are the low efficiency and poor long-term stability. The polymeric membrane has been reported of harvesting electricity from salinity gradient energy (SGE), but it is limited by low power density and complex preparation processes.[9, 10] Recently, a class of membrane materials, namely heterogeneous composite membrane (consisting of a support layer and a thin top layer), has shown great potential to overcome aforementioned obstacles.[11] The asymmetric structure was recognized as an important factor to improve the ion transport feature for energy conversion, separation and water desalination[12]. Besides, polymer composite membranes displayed good flexibility and compatibility compared to porous rigid counterparts, such as porous anodic aluminum oxide (AAO), mesoporous carbons and silica membranes. Combining their low-cost effectiveness and easy fabrication nature, heterogeneous membranes have been considered one of the most promising membrane materials. However, one immediate drawback is the geometric restriction, leading to a significant reduction in membrane performance,[13] including channel tortuosity, narrow transport path and wide size distribution. Taking recent advance of mixed matrix membrane in the development of metal organic framework (MOF) nanosheets, we

expected to mitigate the geometric restriction and hence further improved the membrane performance in the process of SGE conversion.

Here, we reported a new approach to prepare a heterogeneous membrane system by incorporating metal organic framework (MOF) nanosheets as porous fillers into sulfonated polyether ketone (SPEEK) polymer matrix, which was subsequently coated onto a sulfonated polysulfone (SPSF)-based substrate (**Scheme 1**). The presented SPEEK-MOF/SPSF membrane displayed exceptional mechanical stability, tunable ion flux and enhanced energy conversion capability. The incorporation of ultrathin two-dimension (2D) MOFs can increase the ion flow rate in a confinement region within the top layer. In addition, the hierarchical porous structure of the MOF nanosheets will offer a multidimensional pathway along horizontal direction and voids between inorganic-organic interface, which can significantly reduce the geometric restriction effect of the composite configuration. In addition, the output power was further improved by negative temperature gradient (opposite with salinity gradient) at both sides of membrane. This study thus opens up a new avenue for the development of membrane-based technologies for SGE applications.

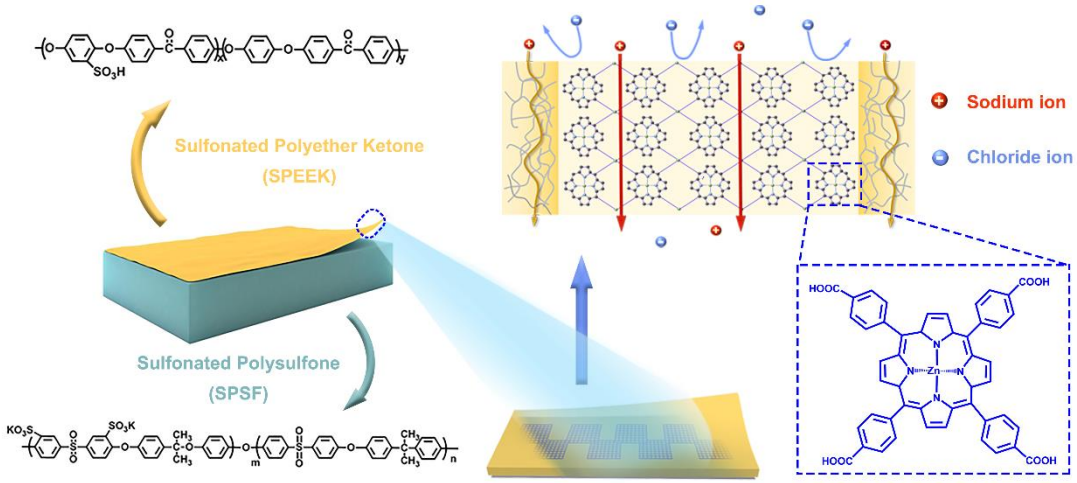

Scheme 1. Composite membrane and its chemical composition. The top layer was SPEEK membrane embed with ZnTCPP MOF and the substrate was SPSF. The addition of 2D nanosheets

could shorten ion transport path.

2. Experimental Section

2.1 Materials

SPEEK and SPSF were purchased from Tianjin Yanjin Technology Co., Ltd. The sulfonation degree was 30%, calculated by ion exchange capacity (IEC) for SPSF. The SPEEK was obtained through concentrated sulfuric acid for 3.5 hours, which sulfonation degree was 85% estimated by NMR (Figure S1)[14]. ZnTCPP nanosheets were synthesized by the solvothermal method. $Zn(NO_3)_2 \cdot 6H_2O$ and polyvinyl pyrrolidone (PVP) were dissolved into the binary solution of DMF and ethanol. Then TCPP was dissolved into binary solution of DMF and ethanol and added to the previous solution dropwise. The solution was transferred into a stainless-steel autoclave at 80°C for 20 h under autogenous pressure. The resultant ZnTCPP nanosheets were washed with ethanol for multiple times and collected by centrifuging (7800 rpm). A heterogeneous membrane was fabricated by a two-pot method. The illustrations were shown in supporting information (Figure S2).

2.2 Characterizations

SEM images were taken in the field-emission mode using Hitachi S-4800. UV-visible absorption spectra were recorded by UV-3600 spectrometer (Shimadzu, Japan). TEM images were captured by the field-emission mode using JEM-2100f. Small-angle X-ray scattering (SAXS) were used by XEUSS, Xenocs, France. AFM was used in a tapping mode (MultiMode 8, Bruke).

Salinity gradient energy conversion tests. The performance of salinity gradient energy conversion was tested with a Keithley 6430 semiconductor picoammeter (Keithley Instruments, Cleveland, OH) using a costumed device. The tested window area was 3×10^{-8} m^2 and a pair of lamellar Ag/AgCl electrode was used. Asymmetric

concentrations of NaCl electrolyte were immersed into the corresponding reservoirs. We simulated the sea water and river freshwater using 50-fold concentration gradient (0.5 M| 0.01 M NaCl).

Localized heating experiments. The light was illumined from the one side of cell (Figure 4a). The wavelength was more than 400 nm. The xenon lamp is kept a distance of 5 cm from the membrane and its power was 50 W. The direction of light illumination is opposite to that of concentration gradient. The temperatures of silicon wafer pairs were tested by thermocouples (Type K calibration, Omega Engineering Inc.).

Permeation experiments. They were performed by a two-cell system separated by membrane. The permeability rate of rhodamine 6G and sulforhodamine were tested separately in order to avoid the interference. The MOF-including side was facing the feed solution and it contained either 0.1 mM rhodamine 6G or sulforhodamine aqueous solution. The permeability was monitored using a spectrofluorophotometer (RF-5301PC, SHIMADZU, Japan).

Conductance test and *I-V* scanning. These two tests were tested with a Keithley 6430 semiconductor picoammeter (Keithley Instruments, Cleveland, OH). The tested area of conductance is 3×10^{-8} m^2 (Figure 2c, d) and that of *I-V* scanning is 1.26×10^{-5} m^2 (Figure 2a and b).

3. Results and Discussion

As a fascinating class of porous crystalline materials, MOFs have been intensively investigated due to their regular and tunable pore structures in the last decade.[15] Particularly, porphyrinic MOF exhibits excellent thermal and chemical stabilities.[16] Compared to 2D MOFs, the three-dimension counterparts usually aggregate in polymer matrix to afford a micro-size particle, which limits their application as fillers in

composite membranes. Building on our early work, ultrathin zinc (II) tetrakis (4carboxy-phenyl) porphyrin) (ZnTCPP) MOF nanosheets were synthesized under a surfactant-assisted solvothermal method[17]. The flexible and transparent nanosheets were then obtained after exfoliation under the assistant of ultrasonication with a thickness of *ca.* 4~5 nm (**Figure 1**a, Figure S3). The pore size of ZnTCPP was estimated at ~1.3 nm,[17] generating from the four-coordinated porphyrin units. The X-ray diffraction (XRD) pattern confirmed the crystalline structure where the dominant peaks centered at 7.6 and 19.4°, representing the miller indices of (002) and (004) (**Figure 1**b). With the MOF nanosheets in hand, we then prepared the ion selective membranes *via* a two-step method. A sulfonated polysulfone (SPSF) solution (in *N*-methyl pyrrolidone, NMP) was casted onto a clear Si wafer and dried at 85 ℃ for 11 hours to afford a substrate. Subsequently, a mixture consisting of sulfonated polyether ketone (SPEEK) and MOF nanosheets in ethanol was spin-coated onto the SPSF substrate. The resultant membrane was immersed into ultrapure water until it peeled off from the wafer automatically. The MOF nanosheets were uniformly dispersed in the mixture under ultrasonic oscillation before spin-coating (Figure S4) and dispersed in SPEEK matrix (Figure S5). The cross-section SEM image revealed the asymmetric structure of the resultant membrane (**Figure 1**c). Specifically, the total thickness of the membrane was 4.3 μm with a SPEEK-MOF mixed matrix top layer of 300 nm (inset of Figure 1a). No clear boundary was observed at the interface between the top layer and the substrate due to their excellent compatibility. Of particular note, multiple spin-coating of the SPEEK-MOF solution (5 times) resulted in an undesirable gutter at the interface due to the mismatched surface tension (Figure S6). What' s more, because of the different exchange rate of solvent and air along vertical direction in the process of solvent evaporation, a denser layer was observed at the bottom of SPSF substrate. The violent

volatilization of solvents (i.e. ethanol) accounted for the rougher surface of top layer. Thus, the AFM Ra and Rq values of SPSF were 0.688 and 0.536 nm while those of SPEEK were 1.02 and 0.815 nm, respectively (**Figure 1**d and e). Because both employed polymer precursors are ionomer components, a distinct phase separation can be observed. For SPEEK, the dark regions represent the hydrophilic phase[18, 19], while the dark regions denote the hydrophobic phase in the case of SPSF[20]. Due to high degree of sulfonation, the ion clusters aggregated leading to the generation of ion domains. The dark regions of SPEEK were spherical with a diameter of 11 to 13 nm (Figure S7) and the ion domains of SPSF were segmentally linear. The hydrophobic portion of the polymer precursor provides mechanical strength and the hydrophilic phase usually forms ion clusters[19], which was further investigated by SAXS (**Figure 1**f and g). We observed double peaks for both SPEEK and SPSF. The *q* values of SPEEK and SPSF were 0.46, 1.42 $Å^{-1}$ and 1.25, 2.91 $Å^{-1}$, respectively. The corresponding ion clusters were 13.65, 4.42 Å and 5.02, 2.16 Å, respectively. Furthermore, the cross-section TEM image of dyed membrane sample indicated different degree of sulfonation between SPSF and SPEEK (Figure S8). The color darkness increased with the sulfonation degree due to the strong electrostatic interaction between sulfonated units and dye molecules. The fabricated membrane possessed unprecedentedly high transmittance despite of MOF incorporating (Figure S9). Notably, the composite membrane possessed good mechanical strength, excellent free-standing and folding features due to the compact polymeric structure. Specifically, a 4 μm-thick, 1 cm-wide membrane sample could hang a weight load of 300 g up (Figure S10). Thermogravimetric analysis (TGA) curves revealed a high thermostability more than 250℃ (Figure S11).

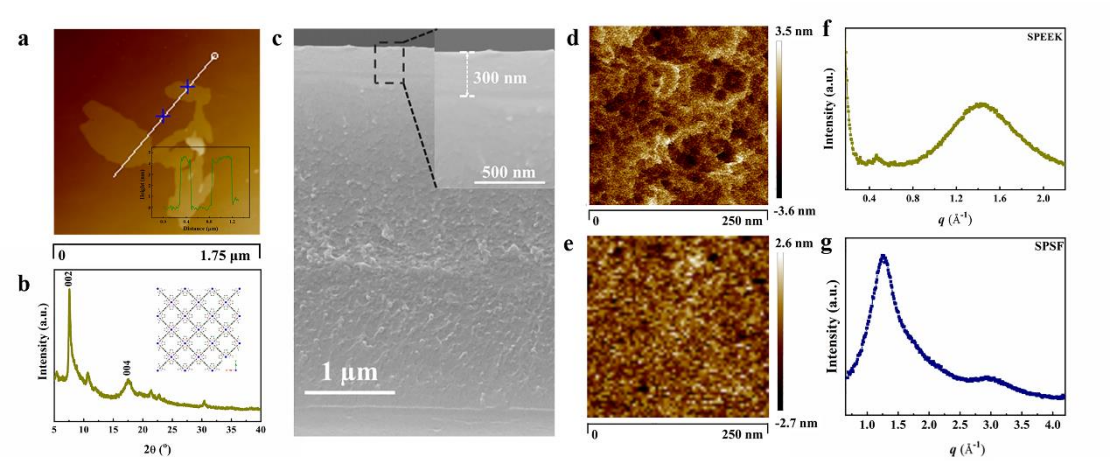

Figure 1. SPEEK-MOF/SPSF composite membrane. (a) AFM image of ZnTCPP and corresponding height profile of ZnTCPP nanosheets. (b) XRD pattern and chemical structure. (c) Cross-section view of SEM image of membrane including its border images with high resolution. (d) and (e) AFM images of pristine SPEEK layer and SPSF layer, respectively. (f) and (g) SAXS patterns of pristine SPEEK layer and SPSF layer, respectively.

We next sought to examine the ion transport performance of the MOF embedding heterogeneous membranes. The pristine SPEEK/SPSF membrane was denoted as M-1, and the MOF incorporating composite membrane was named as M-X (X=2, 3, 4, which corresponds for MOF in terms of wt.% to SPEEK 0.38, 0.73, 1.44). For M-1, no matter at which bias (negative or positive voltage), the obtained current at alkyl electrolyte was far more than that at acid electrolyte (**Figure 2**a). Its pH responsive feature is accounted for the sulfonic groups ($-SO_3H$), which is similar with biological prototype. The stability was estimated by repeated constant voltage scanning (**Figure 2**b). The performance was robust and convincing even if suffering alkali condition. The pH-responsive property and tolerance to extreme condition provide a solid benchmark to potential application. The transmembrane ionic conductance was tested in KCl solution under variable concentrations. The concentration of M-2's conductance deviated from bulk phase was higher than that of M-1. This result suggests more regions are governed by surface charge (**Figure 2**c). The linear *I-V* curves at ultrahigh concentration reveal a

suppressed concentration polarization (CP) effect due to the asymmetric structure (Figure S12).[10] The conductances of different ions were estimated using 0.1 M aqueous solution. Owing to the smaller aperture of ZnTCPP, the conductance of M-2 was less than that of M-1 for Li^+, Na^+ and K^+ ions (**Figure 2**d). The conductances indicated that the nanosheets could reduce inefficient oversized ion channel in the polymetric membrane. The ion selectivity was investigated using Rhodamine (Rh) 6G and sulforhodamine (s-Rh). They have characteristic fluorescence emission spectra and hence their permeabilities were determined by spectrofluorophotomete. The permeability of Rh was higher than that of s-Rh, which indicated that M-2 had cation selectivity due to the negatively charged sulfonic groups (Figure S13).

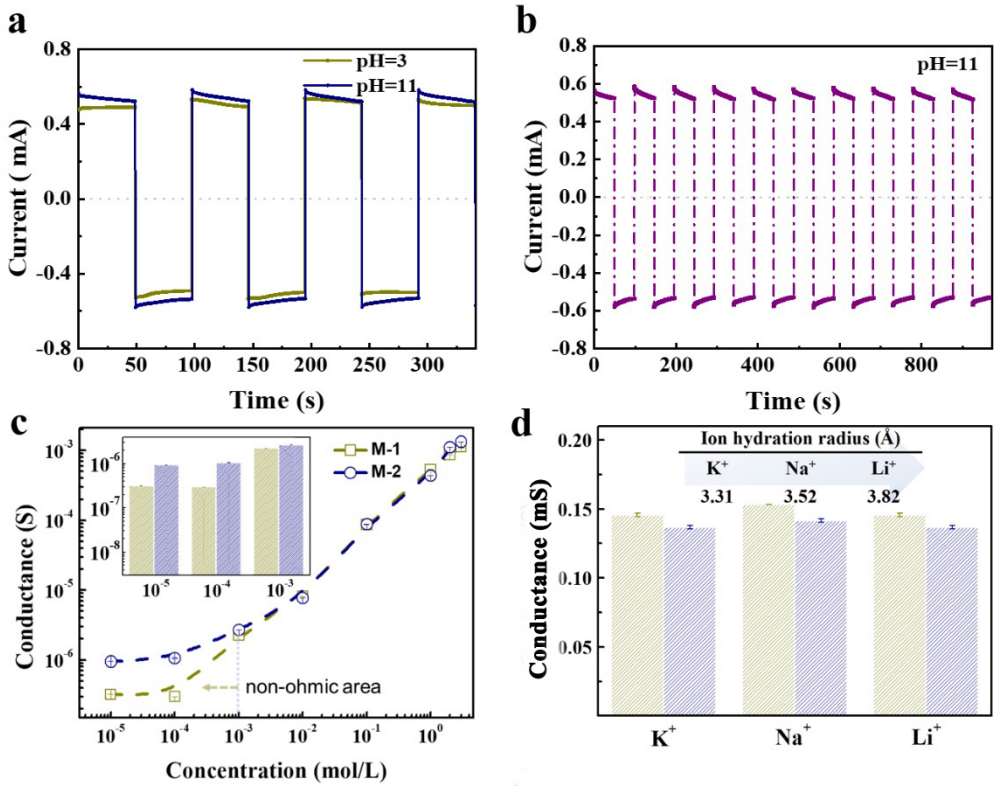

Figure 2. Ion transport property of the presented composite membrane. (a) Ion current of M-1 under different pH stimuli, which means that the ion transport could be regulated by external stimuli like its biological counterpart. (b) The stability of M-1 under pH 11 regulated by voltage. (c) Transmembrane ion conductance of M-1 and M-2. The conductance of M-2 was lower than that of M-1 at high concentration while was higher at low concentration due to the tiny aperture of ZnTCPP (in the inset). (d) Conductances of M-1 and M-2 for different ions.

To benchmark the energy conversion performance, we compared the presented MOF incorporating heterogeneous membrane with other, state-of-the-art flexible membranes. Under 50-fold concentration gradient, the energy conversion performance and power density were investigated. Conventional SPSF membranes displayed an unsatisfactory performance with the open-circuit voltage, short-circuit current and power density of 99 mV, 2.64 μA and 2.7 W m^{-2} respectively, limiting their practical application (Figure S14). In contrast, the power density and current density of the SPEEK/SPSF composite membrane (M-1) increased remarkably by more than one-fold to 5.95 W m^{-2} and 170 A m^{-2}, respectively (**Figure 3**a, b). The free-standing SPEEK membrane were also fabricated, which was obviously weaker than SPEEK/SPSF composite (Figure S15). Thus, the enhanced performance is accounted into the contemplative design of heterogeneity including different sulfonation degree (charge density), pore size distribution and so on. When decreasing the sulfonation degree of SPSF from 35% to 10% or 5%, the collected current reduced dramatically. Because too small sulfonation degree place restrictions on ion flux, the difference in sulfonation degree should be adopted within a proper range (Figure S16). In addition, pore generation strongly depends on the exchange rate of solvent and air during solvent evaporation process. The higher boiling point (bp), the faster would be the exchange rate of solvent and air. We replaced the NMP (bp: 203℃) with a lower boiling point solvent *N, N*-dimethylformamide (DMF, bp: 153℃) and prepared a membrane sample under the same condition. The capability of such membrane was 4.78 W/m^2, weaker than that of M-1 (Figure S17). Theoretically, fast exchange rate would result in the generation of larger pores. Relatively fast volatilization of DMF had a deleterious effect on the pore structure.

Note that once introducing ZnTCPP nanosheets into SPEEK top layer, the power density was enhanced to 6.96 W m^{-2}. The output power increased by about 17% in contrast to pristine composite membrane (M-1). The MOF nanosheets' extremely high porosities, along with direct-passing pore shapes and nanochannel in the interlayer are able to maximize their 2D geometry advantages (Figure S18). The void in the hybrid interfaces may generate multi-dimensional flow in the nanochannel. These advantages could reduce ion transport resistance as well as suppress the geometric restriction effect, meanwhile maintaining the selectivity due to their tiny aperture. The geometric restriction effect often exists in SPEEK membrane, such as channel tortuosity, narrow transport path and wide size distribution. As previously mentioned, the charge density can be enhanced by external pH stimuli. Similar with electric-filed driving force, the ion acceleration can be achieved in the aspect of salinity gradient. A membrane was fabricated half a year ago. We tested power densities of three external load (13000, 17000 and 20000 Ω) and current density of 100 Ω at the condition of pH 11 in **Figure 3**c. The maximal power density could achieve 7.9 W m^{-2}. The composite membrane showed excellent acid and alkali resistant (Figure S19). In order to choose optimized configuration, a 500-fold concentration gradient (5M/0.01M NaCl) was adopted (**Figure 3**d, e). The power densities increased to 24 or 22.57 W m^{-2} for the cases of SPEEK-MOF/SPSF or the opposite SPSF/SPEEK-MOF (to exchange the direction of concentrated side), respectively. The power generation performance was attributed to the designed asymmetric geometry.[21] When the MOF concentration increased, a sharp decrease in energy conversion performance was observed (**Figure 3**g). The open-circuit voltage and short-circuit current decreased from -130.7 to -120.5 or -118.4 mV and the short-circuit current decreased from 6.5 to 6.48 or 3.79 μA, respectively (Figure S20). The corresponding energy conversion efficiency (η) also decreased gradually

(Figure S21, Table S1). When tiny amount of fillers is added, it could distribute uniformly and stack effectively, which are beneficial for improving selectivity.[22-25] Thus, the decreased features can be attributed to two reasons: (1) the random stacking of the excess ultrathin MOF nanosheets lead to pinhole defects and deceased ion selectivity, (2) the flux of stacked nanosheets is less than polymetric membrane with high sulfonation degree.[2] Optimized thickness of top layer could maximize the benefit of heterogeneous structure (Figure S22). Of particular note, the transference number (t_+) of M-2 reached 0.946, representing a high cationic selectivity (Table S2). To emphasis the conversion capability of SGE in this study, we compared the presented SPEEK-MOF/SPSF membrane with the state-of-the-art membranes reported in the literature (**Figure 3**f**,** Table S3).[26-31] Both the energy conversion efficiency (η) and the power density of the presented membrane are the highest comparing all results from these literatures. Indeed, in the assessment of membrane performance many factors should be considered accurately as a prerequisite of high efficiency and low-cost effectiveness.[32, 33] We wish to emphasize here descripting the output power with $P = I \times V$ has become a practice to increase the power density. However, this is an undesirable method since it represents an ideal maximal power which can't be achieved in the real life. A reasonable method could be conducted under the load of external resistance. In addition, a membrane-based generator was constructed to harvest SGE for 96 hours (**Figure 3**h). The obtained current was stable in the long-term testing. The diffusion voltage exhibited a nearly linear relationship with units of power generation in series (**Figure 3**i). Each unit could generate 93 mV diffusion voltage at a concentration gradient of 50.

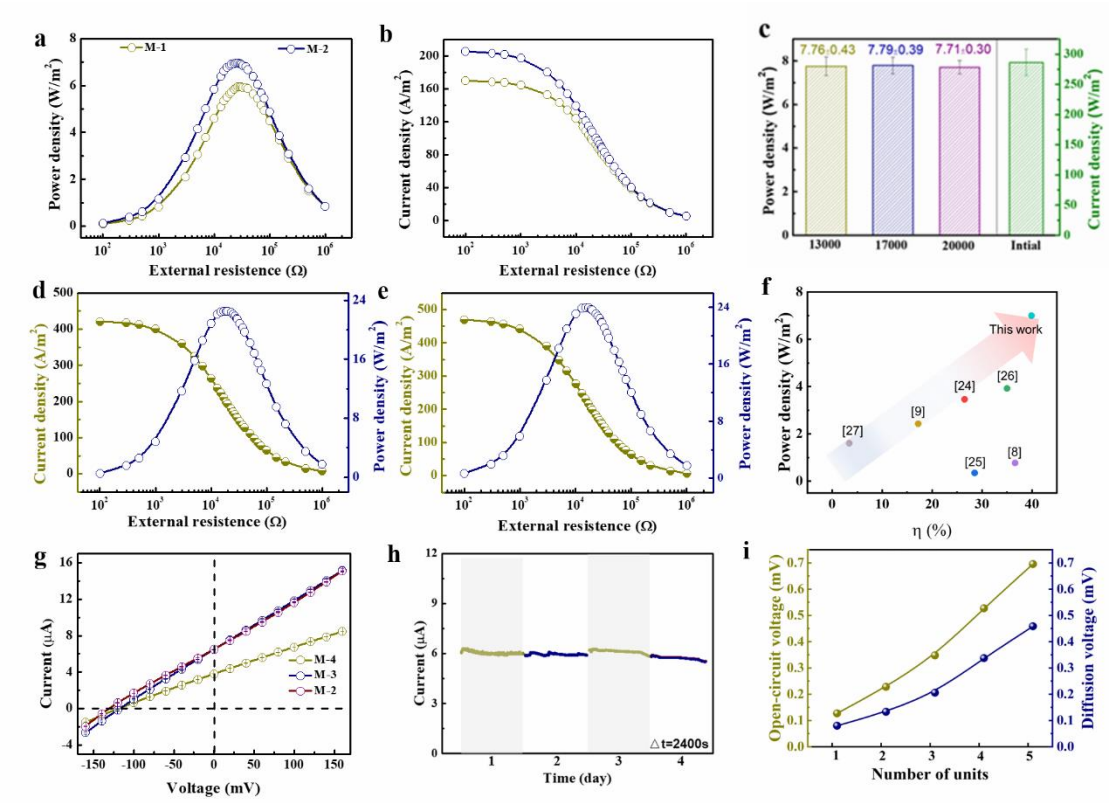

Figure 3. Energy conversion performance. (a) The power density and (b) current density of the composite membrane with or without MOF incorporating. The MOF composite membrane exhibited an enhanced performance at a gradient of 50. (c) Power densities of three external load (13000, 17000 and 20000 Ω) and current density of 100 Ω at the condition of pH 11 and 50-fold concentration gradient. The power generation performance of (d) SPSF/SPEEK-MOF and (e) SPEEK-MOF/SPSF direction at a gradient of 500. (f) Comparison with recent advances to show the superior performance. (g) The *I-V* curves of different membranes under the 50-fold concentration gradient. (h) Long-term stability of the membrane-based generator. (i) The open-circuit voltage and diffusion voltage increase with the units in series.

In order to further improve power generation, we constructed a negative temperature gradient to accelerate power generation (**Figure 4**a). A pair of Si wafer was set tightly on both sides of the membrane. The localized heating was achieved by light illumination at Si wafer through the photothermal effect (**Figure 4**b**,** Figure S23). As shown in **Figure 4**c, the current boosted instantaneously once the light was switched "on", which indicated an accelerated ion transport due to instant temperature gradient. The elevated current (Δ =0.78~0.96 μA) at per circle when the light was switched "on"

was higher than that (α =0.009~0.053 μA) at contiguous circle when the light was switched "off" (**Figure 4**d, Figure S24, Table S4). The current increased by more than 13% compared to pristine current without heating (**Figure 4**e). Obviously, the region of both sides of the membrane was heated preferentially rather than entire bulk phase, confirming that the temperature gradient worked at micro or nano scale. The elevated current was accounted for the Soret effect at charged nano-confined circumstance (Equation S8~10)[34] and augmented diffusion coefficients (Equation S11).[34, 35] When the light was switched, the current increased in comparison with last section. It was because the temperature of both sides increased. In the aqueous solution, high temperature facilitated diffusive coefficients synchronously on both sides of the membrane, thus promoting the ion transportation and membrane potential (Equation S11). Although it has been reported the temperature of solutions played an important role in rapid mass transport for highly efficient energy conversion[34] and the output power could be augmented by the aid of symmetric temperature elevation,[36] increasing the temperature of bulk aqueous phase is energy-intensive and challenging due to extremely high specific heat capacity of aqueous solution. To overcome this disadvantage, the asymmetric temperature was put forward to reduce the energy consumption and boost power generation.[37] Due to the ultrafast heat transfer rate in bulk phase solution, it is very difficult to generate a temperature gradient across the membrane in reality. That's why the light was adopted to subtly construct temperature gradient. We are convinced that this novel design could generate temperature gradient at micro or nano scale and accelerate ion transport, facilitating the power generation and ion transport.

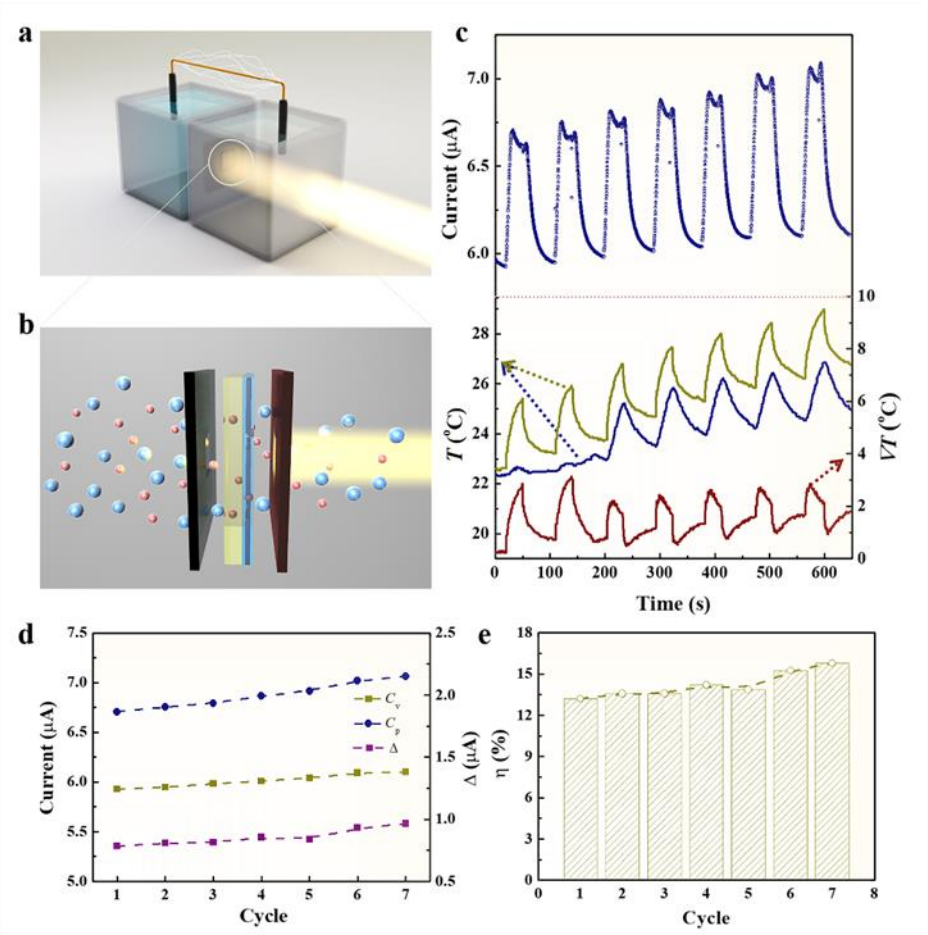

Figure 4. Localized heating. (a) Experiment set-up. The temperature difference was opposite with the salinity gradient. (b) Schematic illustration of the synergetic combination of salinity gradient and temperature difference. The ion diffusion rate accelerated due to negative temperature gradient. (c) Experimental results of multiple cycles. (d) The current values obtained in the "On-Off" experiment. The differences were also calculated. (e) The enhanced current percentage in the "On-Off" experiment, representing the effect of localized heating at each circle.

4. Conclusions

We have successfully fabricated a series of MOF nanosheets incorporating heterogeneous composite membranes. Benefiting from the asymmetry in chemical composition and membrane configuration, the ion transport could be boosted and regulated as required. High performance of SGE conversion attributes the success to MOF nanosheets due to their high porosity originated from long-order crystalline and nanochannel in the interlayer. In addition, taking the advantage of temperature

difference at small-scale region, we developed a new strategy to accelerate ion transport and promote electric generation. Our work thus opens up a new avenue for the development of membrane-based technology for reverse osmosis, nanofiltration, electrodialysis.

Declaration of competing interest

The authors declare no competing financial interest.

Acknowledges

This work was supported by the National Key R&D Program of China (2017YFA0206904, 2017YFA0206900), the National Natural Science Foundation (21625303, 51673206, 21905287, 21988102), Beijing Natural Science Foundation (2194088), the Strategic Priority Research Program of the Chinese Academy of Science (XDA21010213), and the Key Research Program of the Chinese Academy of Sciences (QYZDY-SSW-SLH014). Q.F. acknowledges the funding support form Australian Research Council under Future Fellowship scheme (FT180100312).

REFERENCES

[1] K. Xiao, L. Jiang, M. Antonietti, Ion Transport in Nanofluidic Devices for Energy Harvesting, Joule, (2019) 2364-2380.

[2] Y. Jiang, W. Ma, Y. Qiao, Y. Xue, J. Lu, J. Gao, N. Liu, F. Wu, P. Yu, L. Jiang, L. Mao, Metal‐Organic Framework Membrane Nanopores as Biomimetic Photoresponsive Ion Channels and Photodriven Ion Pumps, Angew. Chem. Int. Edit, 59 (2020) 12795-12799.

[3] R. Li, X. Fan, Z. Liu, J. Zhai, Smart Bioinspired Nanochannels and their Applications in Energy‐Conversion Systems, Adv. Mater., 29 (2017) 1702983.

[4] T.B. Schroeder, A. Guha, A. Lamoureux, G. VanRenterghem, D. Sept, M. Shtein, J. Yang, M. Mayer, An Electric-eel-inspired Soft Power Source from Stacked Hydrogels, Nature, 552 (2017) 214-218.

[5] J. Feng, M. Graf, K. Liu, D. Ovchinnikov, D. Dumcenco, M. Heiranian, V. Nandigana, N.R. Aluru, A. Kis, A. Radenovic, Single-layer MoS_2 Nanopores as Nanopower Generators, Nature, 536 (2016) 1476-4687.

[6] A. Siria, M.-L. Bocquet, L. Bocquet, New Avenues for the Large-scale Harvesting of Blue Energy, Nat. Rev. Chem., 1 (2017) 0091.

[7] S. Balme, T. Ma, E. Balanzat, J.-M. Janot, Large Osmotic Energy Harvesting from Functionalized Conical Nanopore suitable for Membrane Applications, J. Membr. Sci., 544 (2017) 18-24.

[8] M. Macha, S. Marion, V.V. Nandigana, A. Radenovic, 2D Materials as an Emerging Platform for Nanopore-based Power Generation, Nat. Rev. Mater., 4 (2019) 588-605.

[9] X. Huang, Z. Zhang, X.-Y. Kong, Y. Sun, C. Zhu, P. Liu, J. Pang, L. Jiang, L. Wen, Engineered PES/SPES Nanochannel Membrane for Salinity Gradient Power Generation, Nano Energy, 59 (2019) 354-362.

[10] R. Li, J. Jiang, Q. Liu, Z. Xie, J. Zhai, Hybrid Nanochannel Membrane Based on Polymer/MOF for High-performance Salinity Gradient Power Generation, Nano energy, 53 (2018) 643-649.

[11] C. Liu, S. Kulprathipanja, Mixed-Matrix Membranes, John Wiley & Sons, Ltd2010.

[12] X. Zhu, J. Hao, B. Bao, Y. Zhou, H. Zhang, J. Pang, Z. Jiang, L. Jiang, Unique Ion Rectification in Hypersaline Environment: A High-performance and Sustainable Power Generator System, Sci. Adv., 4 (2018) eaau1665.

[13] Z. Zhang, L. He, C. Zhu, Y. Qian, L. Wen, L. Jiang, Improved Osmotic Energy Conversion in Heterogeneous Membrane Boosted by Three-dimensional Hydrogel Interface, Nat. Commun., 11 (2020) 875.

[14] M. Guo, M. Zhang, D. He, J. Hu, X. Wang, C. Gong, X. Xie, Z. Xue, Comb-like Solid Polymer Electrolyte Based on Polyethylene Glycol-grafted Sulfonated Polyether Ether Ketone, Electrochim. Acta, 255 (2017) 396-404.

[15] J. Duan, Y. Li, Y. Pan, N. Behera, W. Jin, Metal-organic Framework Nanosheets: An Emerging Family of Multifunctional 2D Materials, Coord. Chem. Rev., 395 (2019) 25-45.

[16] M. Zhao, Y. Wang, Q. Ma, Y. Huang, X. Zhang, J. Ping, Z. Zhang, Q. Lu, Y. Yu, H. Xu, Ultrathin 2D Metal‐organic Framework Nanosheets, Adv. Mater., 27 (2015) 7372-7378.

[17] M. Liu, K. Xie, M.D. Nothling, P.A. Gurr, S.S.L. Tan, Q. Fu, P.A. Webley, G.G. Qiao, Ultrathin Metal–Organic Framework Nanosheets as a Gutter Layer for Flexible Composite Gas Separation Membranes, ACS Nano, 12 (2018) 11591-11599.
[18] S. Bano, Y.S. Negi, R. Illathvalappil, S. Kurungot, K. Ramya, Studies on Nano Composites of SPEEK/Ethylene Glycol/Cellulose Nanocrystals as Promising Proton Exchange Membranes, Electrochim. Acta, 293 (2019) 260-272.
[19] Q. Zhao, Y. Wei, C. Ni, L. Wang, B. Liu, J. Liu, M. Zhang, Y. Men, Z. Sun, H. Xie, Effect of Aminated Nanocrystal Cellulose on Proton Conductivity and Dimensional Stability of Proton Exchange Membranes, Appl. Surf. Sci., 466 (2019) 691-702.
[20] Z. Qu, H. Wu, Y. Zhou, L. Yang, X. Wu, Y. Wu, Y. Ren, N. Zhang, Y. Liu, Z. Jiang, Constructing Interconnected Ionic Cluster Network in Polyelectrolyte Membranes for Enhanced CO_2 Permeation, Chem. Eng. Sci., 199 (2019) 275-284.
[21] J.-P. Hsu, T.-C. Su, P.-H. Peng, S.-C. Hsu, M.-J. Zheng, L.-H. Yeh, Unraveling the Anomalous Surface-Charge-Dependent Osmotic Power Using a Single Funnel-Shaped Nanochannel, ACS Nano, 13 (2019) 13374-13381.
[22] Y. Meng, L. Shu, L. Liu, Y. Wu, L.-H. Xie, M.-J. Zhao, J.-R. Li, A High-flux Mixed Matrix Nanofiltration Membrane with Highly Water-dispersible MOF Crystallites as Filler, J. Membr. Sci., 591 (2019) 117360.
[23] H. Koulivand, A. Shahbazi, V. Vatanpour, M. Rahmandoust, Development of Carbon Dot-modified Polyethersulfone Membranes for Enhancement of Nanofiltration, Permeation and Antifouling Performance, Sep. Purif. Technol., 230 (2020).
[24] S. Yang, K. Zhang, Few-layers MoS_2 Nanosheets Modified Thin Film Composite Nanofiltration Membranes with Improved Separation Performance, J. Membr. Sci., 595 (2020) 117526.
[25] L. Xu, B. Shan, C. Gao, J. Xu, Multifunctional Thin-film Nanocomposite Membranes Comprising Covalent Organic Nanosheets with High Crystallinity for Efficient Reverse Osmosis Desalination, J. Membr. Sci., 593 (2020) 117398.
[26] J. Gao, W. Guo, D. Feng, H. Wang, D. Zhao, L. Jiang, High-Performance Ionic Diode Membrane for Salinity Gradient Power Generation, J. Am. Chem. Soc., 136 (2014) 12265-12272.
[27] Z. Zhang, X.Y. Kong, K. Xiao, Q. Liu, L. Jiang, Engineered Asymmetric Heterogeneous Membrane: A Concentration-Gradient-Driven Energy Harvesting Device, J. Am. Chem. Soc., 137 (2015) 14765-14772.
[28] J. Ji, Q. Kang, Y. Zhou, Y. Feng, X. Chen, J. Yuan, W. Guo, Y. Wei, L. Jiang, Osmotic Power Generation with Positively and Negatively Charged 2D Nanofluidic Membrane Pairs, Adv. Funct. Mater. , (2017) 1603623.
[29] Z. Zhang, S. Yang, P. Zhang, J. Zhang, G. Chen, X. Feng, Mechanically Strong MXene/Kevlar Nanofiber Composite Membranes as High-performance Nanofluidic Osmotic Power Generators, Nat. Commun., 10 (2019) 1-9.
[30] W. Xin, Z. Zhang, X. Huang, Y. Hu, T. Zhou, C. Zhu, X.-Y. Kong, L. Jiang, L. Wen, High-performance Silk-based Hybrid Membranes Employed for Osmotic Energy Conversion, Nat. Commun., 10 (2019) 1-10.
[31] Z. Zhang, X. Sui, P. Li, G. Xie, X.-Y. Kong, K. Xiao, L. Gao, L. Wen, L. Jiang, Ultrathin and Ion-selective Janus Membranes for High-performance Osmotic Energy

Conversion, J. Am. Chem. Soc., 139 (2017) 8905–8914.
[32] C. Chen, D. Liu, L. He, S. Qin, J. Wang, J.M. Razal, N.A. Kotov, W. Lei, Bio-inspired Nanocomposite Membranes for Osmotic Energy Harvesting, Joule, 4 (2019) 247-261.
[33] Y. Mei, C.Y. Tang, Recent Developments and Future Perspectives of Reverse Electrodialysis Technology: A Review, Desalination, 425 (2018) 156-174.
[34] M. Dietzel, S. Hardt, Thermoelectricity in Confined Liquid Electrolytes, Phys. Rev. Lett., 116 (2016) 225901.
[35] L. Li, Q. Wang, Thermoelectricity in Heterogeneous Nanofluidic Channels, Small, 14 (2018) 1800369.
[36] R. Long, Z. Luo, Z. Kuang, Z. Liu, W. Liu, Effects of Heat Transfer and the Membrane Thermal Conductivity on the Thermally Nanofluidic Salinity Gradient Energy Conversion, Nano Energy, 67 (2020) 104284.
[37] R. Long, Z. Kuang, Z. Liu, W. Liu, Ionic Thermal Up-diffusion in Nanofluidic Salinity Gradient Energy Harvesting, Natl. Sci. Rev., 6 (2019) 1266–1273.

Vitae

Xiaolu Zhao is currently a PhD candidate at the Technical Institute of Physics and Chemistry, Chinese Academy of Sciences (TIPC). He received his B. Eng. Degree and M. Eng. Degree from Harbin Institute of Technology. His current scientific interests are the application of bioinspired nanochannels for energy conversion.

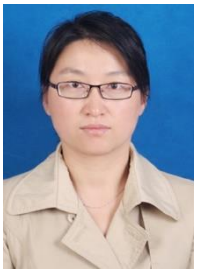

Dr. Chunxin Lu is currently an associate professor in Jiaxing University. She received her Ph.D degree from Zhejiang University. Her scientific interests are the preparation and properties of membrane materials.

Linsen Yang is currently a PhD candidate at the Technical Institute of Physics and Chemistry, Chinese Academy of Sciences (TIPC). He received his B. Eng. Degree from Beihang University. His current scientific interests are the recovery and detection of radioactive elements.

Jianjun chen

Weipeng Chen is currently a PhD candidate at the Technical Institute of Physics and Chemistry, Chinese Academy of Sciences (TIPC). He received his B. Eng. Degree and M. Eng. Degree from Hainan University. His current scientific interests are the construction and application of bioinspired nanochannel membranes.

Weiwen Xin is currently a PhD candidate in Physical Chemistry at the Technical Institute of Physics and Chemistry, Chinese Academy of Sciences (TIPCCAS) under the supervision of Prof. Liping Wen. He received his BS degree in Chemistry (2018) from the Department of Chemistry, Zhengzhou University, and then he joined Prof. Liping Wen's group in 2018. His current scientific interests are focused on asymmetric smart nanochannel membranes for intelligent ion transport control and osmotic energy conversion.

Dr. Xiang-Yu Kong is currently an assistant professor in Prof. Lei Jiang's group

at the Technical Institute of physics and Chemistry, Chinese Academy of Sciences (TIPC). He received his B.Sc. degree from Tianjin University of Science & Technology in 2008. He then received his Ph.D. degree from Institute of Chemistry Chinese Academy of Sciences (ICCAS) in Prof. Wei-Jun Zheng's group. His scientific interest is the biomimetic nanochannels and membrane materials.

Dr. Qiang Fu received his B.E. in chemical engineering from the Shanghai Jiao Tong University in 2004. He completed his Ph.D. in polymer chemistry at the Fudan University in 2009 before working as a Postdoctoral Fellow with Professor Greg Qiao at the University of Melbourne. He was awarded an ARC Super Science Fellowship in 2011 and an ARC Future Fellowship in 2018, respectively. His research interests span from fundamental studies to applied sciences and encompass the fields of two-dimensional polymers, macromolecular engineering and self-assembly, and membrane materials for separations.

Prof. Liping Wen is a Professor at the Technical Institute of Physics and Chemistry, Chinese Academy of Sciences (TIPC). He received his PhD (2010) from ICCAS. He then worked as an Associate Professor in ICCAS. He obtained the National Science Fund for Distinguished Young Scholars in China. His current scientific

interests are the construction and application of bioinspired smart nanochannels and nanopores.

Prof. Greg Qiao

Qiang Fu:

Professor Greg Qiao received his Ph.D. at the University of Queensland in 1996. He joined the University of Melbourne in 1996 and became a full Professor in 2009. He was an Australian Research Council's professorial Future Fellow (2012-2015) and the Chair of Polymer Division of the Royal Australia Chemical Institute (RACI) (2015-2016). He received the Applied Research Award in 2017, ExxonMobil Award in 2015, RACI's Polymer Division Citation in 2011 and Freehills Award in 2010. He has published > 250 journal papers and is a co-inventor of > 20 patents. His key research interests are in polymeric architectures, new activation methods for RAFT, peptide polymers, tissue scaffolds, and gas membranes.

Prof. Lei Jiang is a professor at the Technical Institute of Physics and Chemistry, Chinese Academy of Sciences (TIPCCAS) and Beihang University. He is also an academician of the Chinese Academy of Sciences, Academy of Sciences for the Developing World, and National Academy of Engineering, USA. He has built the interfacial material system with superwettability and further extended this

system to interfacial chemistry. His work pioneers the development of this field, and many of his fundamental technologies have been transferred to practical products in the market.